

Oxygen Evolving complexes- A short Review

Arnab Chatterjee
Basic science and Humanities
Dr.B.C.Roy Polytechnic
Durgapur, India
arnab.chatterjee@brec.ac.in

Souvik De
Basic science and Humanities
Dr.B.C.Roy Polytechnic
Durgapur, India
souvik.de@brec.ac.in

Bholanath Ghosh
Basic science and Humanities
Dr.B.C.Roy Polytechnic
Durgapur, India
bholanath.ghosh@brec.ac.in

Samya Neogi
Basic science and Humanities
Dr.B.C.Roy Polytechnic
Durgapur, India
samya.neogi@brec.ac.in

Ujjal Kar
Basic science and Humanities
Dr.B.C.Roy Polytechnic
Durgapur, India
ujjal.kar@brec.ac.in

Abstract—

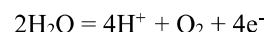
In the 200 years since Joseph Priestley first discovered that green plants replenish “dephlogistated” air by releasing oxygen during illumination, there has not been a more active period than the last few years for investigations of the process of photosynthetic O₂ evolution. This period has been highlighted by major advances in our understanding of the molecular components essential for this process, as well as the application of new probes of the catalytic site. This spurt of activity is founded upon a broad base of knowledge. The material deals with the organization and function of the metal sites implicated in the catalysis of water oxidation during photosynthesis and how they interact with the constituents of Photosystem-II. The following topic deals with the O₂ evolution and role of manganese in O₂ evolution. Photosystem II is a membrane protein located in the thylakoid membrane of oxygen photosynthetic organism like green plants, green algae and cyano bacteria and possesses a number of redox active component which are enable to catalyze the oxidation of water and reduction of plastoquinone .So it performs a series of light induced electron transfer reactions leading to the splitting of water into protons and molecular oxygen, and also water is the source of the electrons that are finally used to convert carbon di-oxide to carbohydrate. The product of PS II, namely chemical energy and molecular oxygen. So it is supplies the oxygen we breath, it maintained the ozone layer needed to protect us from UV radiation and of course it provides the reducing equivalents necessary to fix carbon di-oxide to organic molecule that create biomass, food, and fuel. For these reason it is truly the engine of life and its appearance about 2.5 billion years ago represented the “BIG BANG” of evolution. The light induced oxidation of water is catalysed by a Mn₄Ca cluster, located in the luminal surface of PS II which is denoted as oxygen evolving complex.

Keywords—Oxygen evolving complex, Metal coordination complexes

1. INTRODUCTION

The first hints that manganese is involved in the water splitting-oxygen evolving reaction of PS II system back to the work of Pirson, who showed that Mn deficiency in the fresh water green algae and higher plants inhibited photosynthesis. It was also demonstrated that the inhibition of photosynthesis could be restored by adding back Mn²⁺.

So, Mn was required specifically for the water splitting reaction began with the work of Kessler et al, who noted that Mn deficiency in algae resulted in a reduction in the level of luminescence and this effect coincided with the inhibition of photosynthesis. However they found under the same condition that the photoreduction of CO₂ using H₂ as an electron source was not inhibited. The explanation of this result became clear with the emergence of the concept of two photosystem acting in series indicating that Mn ions were needed for the oxygen evolving activity of PS II but not for light induced electron transport through PS I. So, when four electrons and four protons are extracted from two molecules of water, one molecule of di-oxygen is formed.



The reaction requires the energy of four photons.

2. OVERALL STRUCTURE

The overall structure is shown in Fig. 1. Every PSII monomer contains 19 protein subunits, among which PsbY was not found, suggesting that this subunit has been lost during purification or crystallization, presumably owing to its loose association with PSII4 - 8. In addition to the protein subunits, there were 35 chlorophylls, two pheophytins, 11 b-carotenes, more than 20 lipids, two plastoquinones, two haem irons, one non-haem iron, four manganese atoms, three or four calcium atoms (one of which is in the Mn₄Ca cluster), three Cl⁻ ions (two of which are in the vicinity of the Mn₄Ca cluster), one bicarbonate ion and more than 15 detergents in a monomer. Within each PSII monomer, more than 1,300 water molecules were found, yielding a total of 2,795 water molecules in the dimer. As shown in Fig., the water molecules were organized into two layer located on the surfaces of the stromal and luminal sides, respectively, with the latter having more water molecules than the former. A few water molecules were found within the membrane region, most of them serving as ligands to chlorophylls (see below).

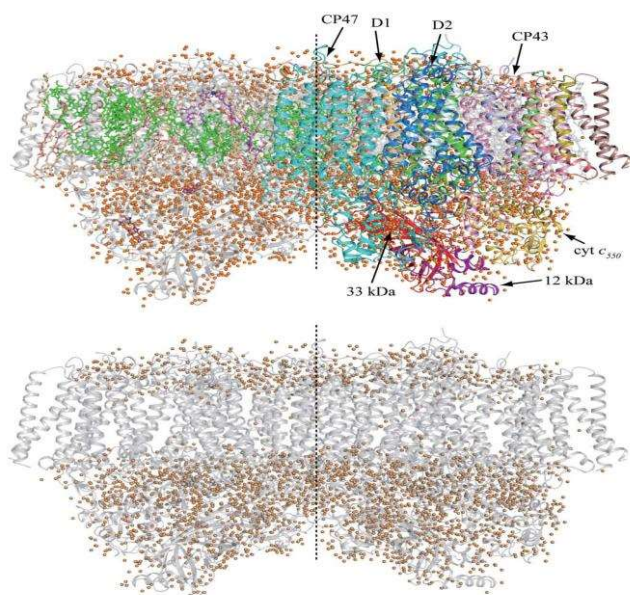


Fig.1: Overall structure of PSII dimer at a resolution of 1.9 Å

View from the direction perpendicular to the membrane normal.

- Overall structure. The protein subunits are coloured individually in the righthand monomer and in light grey in the left-hand monomer, and the cofactors are coloured in the left-hand monomer and in light grey in the right-hand monomer. Orange balls represent water molecules.
- Arrangement of water molecules in the PSII dimer.

The protein subunits are coloured in light grey and all other cofactors are omitted. The central broken lines are the noncrystallographic two-fold axes relating the two monomers.

2.1 STRUCTURE OF Mn_4CaO_5 CLUSTER

The electron densities of the four manganese atoms and the single calcium atom in the oxygen-evolving complex were well defined and clearly resolved, and the electron density for the calcium atom was lower than those of the manganese atoms, allowing us to identify the individual atoms unambiguously (Fig. 2a). In addition, five oxygen atoms were found to serve as oxo bridges linking the five metal atoms. This gives rise to a Mn_4CaO_5 cluster. Of these five metals and five oxygen atoms, three manganese, one calcium and four oxygen atoms form a cubane-like structure in which the calcium and manganese atoms occupy four corners and the oxygen atoms occupy the other four. The bond lengths between the oxygens and the calcium in the cubane are generally in the range of 2.4 – 2.5 Å, and those between the oxygens and Manganese atoms are in the range of 1.8 – 2.1 Å (Fig. 2b). However, the bond length between one of the oxygens at the corner of the cubane (O5) and the calcium is 2.7 Å, and those between O5 and the Manganese atoms are in the range of 2.4 – 2.6 Å. Owing to these differences in bond lengths, the Mn_3CaO_4 cubane is not an ideal, symmetric one. The fourth manganese (Mn4) is

located outside the cubane and is linked to two Manganese atoms oxygen (O4) by a di- μ -oxo bridge. In this way, every two adjacent Manganese atoms are linked by di- μ -oxo bridges: Mn1 and Mn2 are linked by a di- μ -oxo bridge via O1 and O3, Mn2 and Mn3 are linked via O2 and O3, and Mn3 and Mn4 are linked via O4 and O5. The calcium is linked to all four Manganese atoms by oxo bridges: to Mn1 via the di- μ -oxo bridge formed by O1 and O5, to Mn2 via O1 and O2, to Mn3 via O2 and O5, and to Mn4 via the mono- μ -oxo bridge formed by O5. The whole structure of the Mn_4CaO_5 cluster resembles a distorted chair, with the asymmetric cubane serving as the seat base and the isolated Mn4 and O4 serving as the back of the chair. The distances among the four Manganese atoms determined for monomer are 2.8 Å (Mn1 – Mn2), 2.9 Å (Mn2 – Mn3), 3.0 Å (Mn3 – Mn4), 3.3 Å (Mn1 – Mn3) and 5.0 Å (Mn1 – Mn4) (Fig. 2c). The distances between the calcium and the four Manganese atoms are 3.5 Å (Ca – Mn1), 3.3 Å (Ca – Mn2), 3.4 Å (Ca – Mn3) and 3.8 Å (Ca – Mn4) (Fig. 2d). In addition to the five oxygens, four water molecules (W1 to W4) were found to be associated with the Mn_4CaO_5 cluster, of which W1 and W2 are coordinated to Mn4 with respective distances of 2.1 and 2.2 Å, and W3 and W4 are coordinated to the calcium with a distance of 2.4 Å. No other water molecules were found to associate with the other three Manganese atoms, suggesting that some of the four waters may serve as the substrates for water oxidation. All of the amino-acid residues coordinated to the Mn_4CaO_5 cluster were identified (Fig. 2e). Of these, D1-Glu 189 (D1 is one of the reaction centre subunits of PSII), served as a monodentate ligand to Mn1. All of the remaining five carboxylate residues served as bidentate ligands: D1-Asp 170 as a ligand to Mn4 and Ca, D1-Glu 333 to Mn3 and Mn4, D1-Asp 342 to Mn1 and Mn2, D1-Ala 344 (the carboxy-terminal residue of D1) to Mn2 and Ca, and CP43-Glu 354 to Mn2 and Mn3 (CP43 is one of the core antenna subunits of PSII). In addition, D1-His 332 is coordinated to Mn1, whereas D1-His 337 is not directly coordinated to the metal cluster. Most of the distances of the ligands to Manganese atoms are in the range of 2.0 – 2.3 Å; the two shortest distances are 1.9 Å, between D1-Glu 189 and Mn1, and 2.0 Å, between D1-Ala 344 and Mn2. The distances of two carboxylate ligands to the calcium, D1-Asp 170 and D1-Ala 344, are slightly longer (2.3 – 2.4 Å) than the ligand distances to the Manganese atoms. Combining with the oxo bridges and waters, these give rise to a saturating ligand environment for the Mn_4CaO_5 cluster: each of the four Manganese atoms has six ligands whereas the calcium has seven ligands. The ligation pattern and the geometric positions of the metal atoms revealed in the present structure may have important consequences for the mechanisms of water splitting and O – O bond formation. In addition to the direct ligands of the Mn_4CaO_5 cluster, we found that D1-Asp 61, D1-His 337 and CP43-Arg 357 are located in the second coordination sphere and may have important roles in maintaining the structure of the metal cluster. One of the guanidinium η -nitrogens of CP43-Arg 357 is hydrogen-bonded to both O2 and O4 of the Mn_4CaO_5 cluster, whereas the other is hydrogen-bonded to the carboxylate oxygen of D1-Asp 170 and to that of D1-Ala 344. The imidazole nitrogen of D1-His 337 is hydrogen-bonded to O3. These

two residues may thus function to stabilize the cubane structure of the metal cluster as well as to provide partial positive charges to compensate for the negative charges induced by the oxo bridges and carboxylate ligands of the metal cluster. The carboxylate oxygen of D1-Asp 61 is hydrogen-bonded to W1, and also to O4 indirectly through another water molecule, suggesting that this residue may also contribute to stabilizing the metal cluster. Furthermore, D1-Asp 61 is located at the entrance of a proposed proton exit channel involving a chloride ion (Cl21; see below), suggesting that this residue may function in facilitating proton exit from the Mn_4CaO_5 cluster.

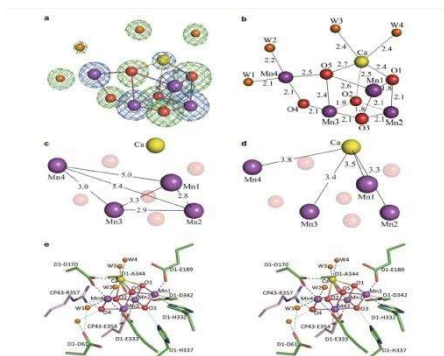


Fig.2: Structure of the Mn_4CaO_5 cluster

- Determination of individual atoms associated with the Mn_4CaO_5 cluster.
- Distances (in angstrom unit) between metal atoms and oxo bridges or water molecules.
- Distances between each pair of manganese atoms.
- Distances between the manganese and the calcium atoms.
- Stereo view of the Mn_4CaO_5 cluster and its ligand environment.

The distances shown are the average distances between the two monomers. Manganese: purple; calcium: yellow; oxygen: red; D1: green; CP43: pink.

2.2 HYDROGEN-BOND NETWORK AROUND Y_Z

Y_Z is located between the Mn_4CaO_5 cluster and the PSII reaction centre, and functions to mediate electron transfer between the two. We found an extensive hydrogen-bonding network between Y_Z and the Mn_4CaO_5 cluster and from Y_Z to the luminal bulk phase. Y_Z was hydrogen-bonded to the two waters coordinated to the calcium either directly (W4) or indirectly through another water (W3; Fig. 3a). The hydrogen bond between the additional water and Y_Z that mediates the link from W3 to Tyr161 has a length of 2.6\AA , suggesting that this is a strong hydrogen bond. This additional water also mediates the hydrogen bond between the two waters bound to Mn_4 and Y_Z . Furthermore, another strong hydrogen bond was found between Y_Z and the nitrogen of D1-His 190, which is 2.5\AA in length and lies on the opposite side of the Mn_4CaO_5 cluster. D1-His 190 was further hydrogen-bonded to D1-Asn 298 and to several waters and residues including CP43-Ala 411, D1-Asn 322 and PsbV-Tyr 137 (the C-terminal residue of the PsbV subunit), leading to an exit pathway to the luminal bulk solution (Fig. 3b). This hydrogen-bond network is located in

the interfaces between the D1, CP43 and PsbV subunits and may function as an exit channel for protons that arise from PCET via Y_Z . This provides support for the existence of a PCET pathway involving Y_Z and D1-His 190, as implied by a number of previous studies^{23–25}. PsbV-Tyr 137, at the exit of this channel, is surrounded by several charged residues including D1-Arg 323, D1-His 304 and PsbV-Lys 129; these residues may therefore function to regulate the proton excretion through the PCET pathway (Fig. 3b). The other redox-active tyrosine residue, YD (D2-Tyr 160), has a different, rather hydrophobic, environment from that of Y_Z . For a discussion of the environment of YD, see Supplementary Fig. 3 and discussions.

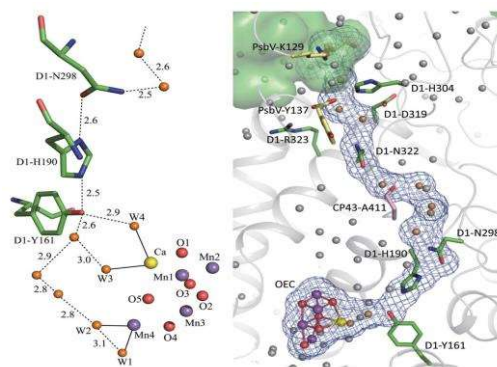


Fig.3:| Hydrogen-bond network around Y_Z

- Hydrogen bonds around Y_Z (D1-Tyr 161). The bonds between metal atoms and water ligands are depicted as solid lines, and the hydrogen bonds are depicted as dashed lines. Distances are expressed in angstrom.
- Hydrogen-bond network from the Mn_4CaO_5 cluster through Y_Z to the luminal bulk phase. Water molecules participating in the hydrogen-bond network are depicted in orange, whereas those not participating are depicted in grey. The area in green in the upper left corner represents the luminal bulk surface. PsbV, pale yellow.

2.3. THE STRUCTURE AND BINDING OF CHLORIDE-BINDING SITE

In the present study, the electron density for the two Cl⁻-binding sites were clearly visible (Fig. 4a), which were confirmed from the anomalous difference Fourier map calculated with data collected at a wavelength of 1.75\AA (Fig. 4a). The two Cl⁻-binding sites are located in the same position as those reported for Br⁻- or I⁻-substituted PSII previously^{26,27} (Fig. 4b, c). Both Cl⁻ ions are surrounded by four species, among which two are waters. For one of the ions, Cl21, the other two species are the amino group of D2-Lys 317 and the backbone nitrogen of D1-Glu 333, and for the other ion, Cl22, they are the backbone nitrogens of D1-Asn 338 and CP43-Glu 354. Because the side chains of D1-Glu 333 and CP43-Glu 354 are coordinated to the Mn_4CaO_5 cluster directly, the two Cl⁻ anions may function to maintain the coordination environment of the Mn_4CaO_5 cluster, thereby allowing the oxygen-evolving reaction to proceed properly.

In addition to the structural roles, the two Cl⁻-binding sites were found to lie at the entrance of hydrogen-bond networks starting from the Mn_4CaO_5 cluster and extending

towards the luminal bulk solution (Fig. 4b, c). The network through Cl21 was located in the interface of the D1, D2 and PsbO subunits, and that through Cl22 was located in the interface of the D1, CP43 and PsbU subunits. These hydrogen-bond networks involve a number of bound waters and some hydrophilic or charged amino-acid residues; they thus may function as either proton exit channels or water inlet channels.

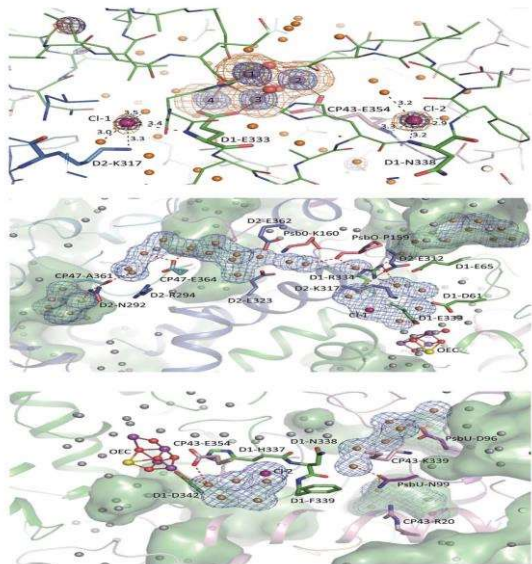


Fig 4. Structure of two Cl₂-binding sites.

- Location of the two Cl₂ ions
- Hydrogen-bond network from the Mn₄CaO₅ cluster through the Cl₂1-binding site to the luminal bulk phase
- Hydrogen-bond network from the Mn₄CaO₅ cluster through the Cl₂2-binding site to the luminal bulk phase.

2.3 CHLOPHYLLS AND β-CAROTENES

We determined the ligands to the central magnesium of all of chlorophylls, of which seven are coordinated by water instead of amino-acid residues (Fig. 5a). These are Chl6 (the accessory chlorophyll of D1); Chl7 (the accessory chlorophyll of D2); Chl12, Chl18 and Chl21, harboured by CP47; and Chl-31 and Chl-34, harboured by CP43. In addition, Chl38 was coordinated by CP43-Asn 39 and all other chlorophylls are coordinated by histidines. From our electron density map, we confirmed that all of the C8 and C13 positions in the phytol chains have a (R, R) configuration, in agreement with the stereochemistry determined for the complete phytol chain^{28,29}. Furthermore, we found that most of the vinyl groups are located in or near the same plane of the tetrapyrrole ring, which may contribute to the extension of energy coupling within the plane and hence facilitate the energy migration between adjacent chlorophylls.

3. CHARGE SEPARATION AND ELECTRON TRANSFER IN PS II

A range of biochemical and biophysical techniques had provided a good understanding of the events that give rise to the primary and secondary electron-transfer processes leading to water oxidation. These processes are initiated by the absorption of light energy by the many chlorophyll and other pigment molecules associated with PSII. The nature of these PSII light-harvesting antenna systems varies under different growth conditions and with different types of organisms. However, within the PSII core complex, only chlorophyll a (Chl a) and β-carotene are found, bound mainly to the CP43 and CP47 proteins (Fig.5). In total, there are about 36 Chl a and 11 β-carotene molecules per PSII core based on biochemical⁴ and structural analyses.

The excitation energy absorbed by these pigments is transferred to the reaction center (RC) composed of the D1 and D2 proteins. Together these RC proteins bind all of the redox-active cofactors involved in the energy conversion process, and the following sequence of reactions occurs. A special form of Chl a, P, acts as an exciton trap and is converted to a strong reducing agent after excitation (P*). P* reduces a pheophytin molecule (Pheo) within a few picoseconds to form the radical pair state P•+Pheo•-. Within a few hundred picoseconds, Pheo•- reduces a firmly bound plastoquinone (PQ) molecule protein (QA) to produce P•+PheoQA•-. P•+, which has a very high redox potential (>1 V), oxidizes a tyrosine residue (TyrZ) to form TyrZ•+PheoQA•-. The neutral tyrosine radical (TyrZ•) is formed because a deprotonation of its phenolic group is concomitant with its oxidation by P•+. In the millisecond time domain, QA•- reduces a second PQ (QB) to form TyrZ•+PheoQAQB•-. At about the same time, TyrZ• extracts an electron from a cluster of four Mn atoms that bind the two substrate water molecules. A second photochemical turnover reduces QB•- to QB²⁻, which is then protonated to plastoquinol and released from PSII into the lipid bilayer, subsequently oxidized by photosystem I (PSI) via the cytochrome b6f complex. Two further photochemical turnovers provide a cluster of four Mn ions and a Ca ion (Mn₄Ca) with a total of four oxidizing equivalents, which are used to oxidize two water molecules to dioxygen. Each oxidation state generated in the oxygen-evolving complex (OEC) is represented as an intermediate of the S-state cycle^{9,10} of which there are five (S₀–S₄). In addition to these reactions, side reactions can occur under some conditions including the oxidation of a high potential cytochrome bound within the PSII core complex (Cyt b559), a β-carotene molecule, and a Chl a molecule (ChlZ)^{11–13} (Fig). These side reactions occur on the tens of millisecond time scale and therefore do not compete with the electron-transfer pathway leading to water oxidation. Indeed, they probably only occur when the rate of water oxidation becomes limited and thus provide a protective mechanism against the detrimental reactions resulting from the very high redox potential of the long-lived P radical cation.

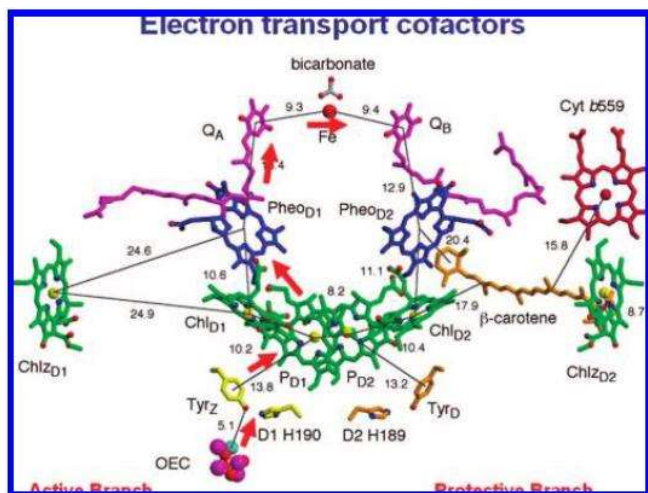


Fig. 5. Electron Transport

4. MECHANISM OF O-O BOND FORMATION IN THE OEC OF PS II

Despite numerous experimental and theoretical model studies, the actual mechanism for the formation of molecular oxygen is not clear. In principle, three different mechanisms have been suggested for the formation of the O-O bond:

- nucleophilic attack of water or hydroxide on a formally MnV species
- radical coupling of two Mn(V) oxo species
- radical coupling of water (or hydroxide) with a bridging oxygen in the manganese cluster.

Between these nucleophilic attack of water or hydroxide on a Mn(v) species is energetically more favourable.

To get experimental evidence for a mechanism involving nucleophilic addition, we decided to study the reaction between a $Mn^v=O$ corrole species and hydroxide ion. At first Mn(III)-corrole complex is prepared by the reaction of 5,10,15-tris(4-nitrophenyl) corrole with $Mn(OAc)_2 \cdot 4H_2O$ in refluxing DMF.

First, the Mn(III) corrole complex **1** is oxidized to the Mn(V) oxo complex **2**.

Second, nucleophilic attack of hydroxide presumably gives initially the Mn(III) hydroperoxy complex **3**. This is oxidized (e.g., by unreacted MnV oxo complex) to give the Mn(IV) hydroperoxy complex, which after loss of a proton gives rise to the observed peroxy complex **4**. This either disproportionates with loss of oxygen or is oxidized to the corresponding MnV complex, which undergoes reductive elimination of oxygen to form the starting complex **1**.

The main conclusion from this study is that O-O bond formation via nucleophilic attack of hydroxide on a Mn(V) oxo oxygen has been experimentally demonstrated and is a possible mechanism for conversion of water into molecular oxygen.

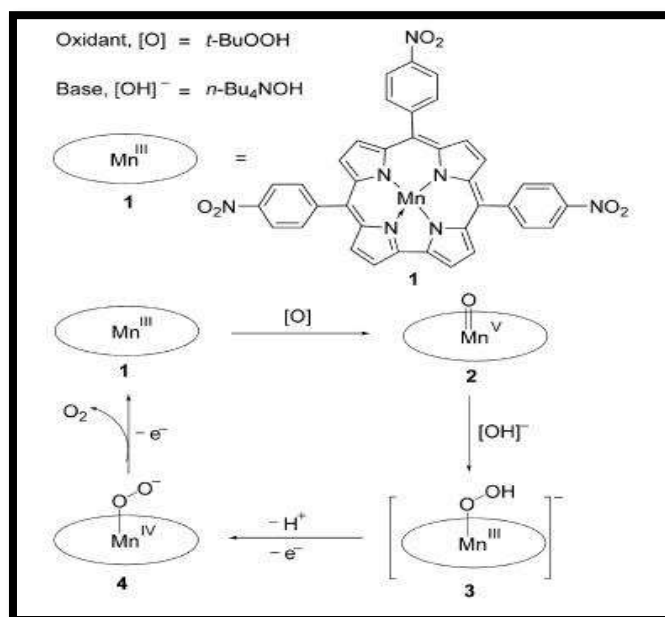


Fig.6. Probable mechanism of the oxygen evolution cycle

5. CONCLUSION

The structure of PSII reveals the geometric arrangement of the Mn_4CaO_5 cluster as well as its oxo bridges and ligands, and four bound water molecules. This provides a basis for the mechanism of water splitting and O-O bond formation, one of nature's most fascinating and important reactions. In addition, water oxidation chemistry has garnered greater importance as the oxidizing half of a "Hydrogen Economy". To ecologically and economically burn H_2 , using O_2 , one should couple hydrogen production to dioxygen production from water. When such catalytic advances are made, we will not only have conquered one of the most challenging chemical reactions in nature, but also have taken a step toward generating new energy sources to sustain our civilization.

ACKNOWLEDGMENT

The authors would like to acknowledge Dr. B. C. Roy Polytechnic for providing the necessary infrastructure.

REFERENCES

- R. M. Cinco, K. L. M. Holman, J. H. Robblee, Junko Yano, S. A. Pizarro, E. Bellacchio, K. Sauer, and V. K. Yachandra, "Calcium EXAFS establishes the Mn-Ca cluster in the oxygen-evolving complex of Photosystem", *Biochemistry*, vol. 41, pp 12928-12933, 2002.
- S. Styring and A. W. Rutherford, "In the oxygen-evolving complex of photosystem II the S_0 state is oxidized to the S_1 state by D^+ (signal IIslow)" *J. Am. Chem. Soc.*, vol. 26(9) pp 2401-2405, 1987.
- J. G. Metz, P. J. Nixon, M. Rogner, G. W. Brudvig, and B. A. Diner, "Directed alteration of the D1 polypeptide of photosystem II: evidence that tyrosine-161 is the redox component, Z, connecting the oxygen-evolving complex to

- the primary electron donor, P680", *Biochemistry*, vol.28(17), pp 6960-6969, 1989.
4. N. Ohnishi, S. I. Allakhverdiev, S. Takahashi, S. Higashi, M. Watanabe, Y. Nishiyama, and N. Murata, "Two-Step Mechanism of Photodamage to Photosystem II: Step 1 Occurs at the Oxygen-Evolving Complex and Step 2 Occurs at the Photochemical Reaction Center", *Biochemistry*, vol. 44(23), pp 8494-8499, 2005
 5. J. Messinger, J. H. Robblee, W. O. Yu, K. Sauer, V. K. Yachandra, and M. P. Klein, "The S₀ State of the Oxygen-Evolving Complex in Photosystem II Is Paramagnetic: Detection of an EPR Multiline Signal", *J. Am. Chem. Soc.*, vol. 119(46), pp 11349-11350, 1997.
 6. K. A. Åhrling, S. Peterson, and S. Styring, "The S₀ state EPR signal from the Mn cluster in photosystem II arises from an isolated S = 1/2 ground state" *Biochemistry*, vol. 37(22), pp 8115–8120, 1998.
 7. R.D Britton, K. A. Campbell, J. M. Peloquin, M. L. Gilchrist, C. P. Aznar, M. M. Dicus, J. Robblee, J. Messinger, "Recent pulsed EPR studies of the Photosystem II oxygen-evolving complex: implications as to water oxidation mechanisms" *Biochimica et Biophysica Acta (BBA) – Bioenergetics*, vol. 1655, pp 158–171, 2004.
 8. L. Iuzzolino, J. Dittmer, W. Dörner, W. M. Klauke, and H. Dau, "X-ray Absorption Spectroscopy on Layered Photosystem II Membrane Particles Suggests Manganese-Centered Oxidation of the Oxygen-Evolving Complex for the S₀-S₁, S₁-S₂, and S₂-S₃ Transitions of the Water Oxidation Cycle" *Biochemistry*, vol. 37(49), pp 17112-17119, 1998
 9. J. L. Zimmermann and A. W. Rutherford, "Electron paramagnetic resonance properties of the S₂ state of the oxygen-evolving complex of photosystem II", *Biochemistry* vol. 25(16), pp 4609-4615, 1986.
 10. X. S. Tang, D. W. Randall, D. A. Force, B. A. Diner, and R. D. Britt, "Manganese-Tyrosine Interaction in the Photosystem II Oxygen-Evolving Complex", *J. Am. Chem. Soc.*, vol. 118, pp 7638-7639, 1996
 11. S. L. Dexheimer and M. P. Klein, "Detection of a paramagnetic intermediate in the S₁ state of the photosynthetic oxygen-evolving complex" *J. Am. Chem. Soc.*, vol. 114(8), pp 2821-2826, 1992
 12. G. C. Papageorgiou & N. Murata, "The unusually strong stabilizing effects of glycine betaine on the structure and function of the oxygen-evolving Photosystem II complex", *Photosynthesis Research* vol.44, pp 243-252, 1995.
 13. F. Liu, J. J. Concepcion, J. W. Jurss, T. Cardolaccia, J. L. Templeton, and T. J. Meyer, "Mechanisms of Water Oxidation from the Blue Dimer to Photosystem II" *Inorg. Chem.*, vol. 47 (6), pp 1727-1752, 2008.
 14. J. Barber, "Crystal Structure of the Oxygen-Evolving Complex of Photosystem II." *Inorg. Chem.*, vol. 47, pp 1700-1710, 2008.
 15. J. Raymond, R. E. Blankenship, "The origin of the oxygen-evolving complex" *Coordination Chemistry Reviews*, vol. 252(3-4), pp 377–383, 2008
 16. J. Barber, J. W. Murray, "Revealing the structure of the Mn-cluster of photosystem II by X-ray crystallography" *Coordination Chemistry Reviews* vol. 252(3-4) pp 233–243, 2008
 17. L. V. Kulik, B. Epel, Wolfgang Lubitz,* and Johannes Messinger, "⁵⁵Mn Pulse ENDOR at 34 GHz of the S₀ and S₂ States of the Oxygen-Evolving Complex in Photosystem II", *J. Am. Chem. Soc.*, vol. 127(8), pp 2392-2393, 2005.
 18. J. Yano, Y. Pushkar, P. Glatzel, A. Lewis, K. Sauer, J. Messinger, U. Bergmann, and V. Yachandra, "High-Resolution Mn EXAFS of the Oxygen-Evolving Complex in Photosystem II: Structural Implications for the Mn₄Ca Cluster", *JACS*, vol. 127(43), pp 14974-14975, 2005.
 19. Y. Umena, K. Kawakami, J. R. Shen & N. Kamiya, "Crystal structure of oxygen-evolving photosystem II at a resolution of 1.9 Å", *NATURE*, vol. 473, pp 55-62, 2011.
 20. A. K. Poulsen, A. Rompel, and C. J. McKenzie, "Water Oxidation Catalyzed by a Dinuclear Mn Complex: A Functional Model for the Oxygen-Evolving Center of Photosystem II", *Angew. Chem.*, vol. 117, pp 7076–7080, 2005.